

# Parametric Resonance in a Model of Cochlear Dynamics

William Ko<sup>1,b)</sup> and John M. Stockie<sup>2,a)</sup>

<sup>1</sup>*Department of Mathematical Sciences, University of Cincinnati, 2815 Commons Way,  
Cincinnati, OH, 45221-0025, USA*

<sup>2</sup>*Department of Mathematics, Simon Fraser University, 8888 University Drive, Burnaby, BC, V5A 1S6, Canada*

<sup>a)</sup>Corresponding author: stockie@math.sfu.ca

<sup>b)</sup>william.ko@uc.edu

**Abstract.** The remarkable ability of the cochlea to amplify sound signals is understood to derive in part from an active process that magnifies vibrations of the basilar membrane and cochlear partition in which it is embedded. This phenomenon is commonly attributed to some form of mechanical resonance within the cochlea, supported by experiments showing that outer hair cells change length when stimulated, thereby causing periodic distortions of the basilar membrane and other cochlear structures. This mechanical amplification is sufficient to overcome the relatively large viscous damping from the surrounding cochlear fluid. Numerous mathematical modelling studies support this hypothesis, although most either ignore or over-simplify the underlying fluid dynamics. Furthermore, there remains as yet no consensus regarding the precise causes of cochlear amplification.

Our aim is to investigate the impact of fluid-structure interaction on cochlear dynamics, inspired by recent results on resonant interactions between an elastic membrane and a viscous fluid. We develop an immersed boundary model for the basilar membrane wherein small-amplitude periodic internal forcing due to oscillatory outer hair cell motion can induce parametric resonance. A Floquet stability analysis demonstrates the existence of resonant (unstable) solutions for physical parameters corresponding to mammalian auditory systems, and also exhibits travelling wave solutions that are consistent with other models. Numerical simulations validate our analytical results and identify fluid-mediated resonant effects as a possible contributing mechanism in cochlear mechanics that we advocate should be considered in modelling studies of the active process.

## INTRODUCTION

Sound waves entering the outer ear are transferred to the cochlear duct by the stapes, which generates travelling waves that propagate along the basilar membrane (BM) while also simultaneously exciting the surrounding cochlear fluid. The cochlea has a remarkable ability to amplify the weak BM oscillations and hence overcome the strong viscous damping effects of the fluid [7], an ability that many authors have attributed to some active cellular process or resonant forcing mechanism arising from the complex structure of the cochlear partition [2, 4, 8, 17]. A second defining feature of the cochlea is its fine frequency tuning ability that distinguishes between different sound frequencies by localizing the peak amplitude of travelling waves along the BM. Despite recent progress in the understanding of cochlear mechanics, there remain many open questions and there is still no consensus regarding the precise causes of cochlear amplification [1, 2, 18].

Many mathematical models of the cochlea have been proposed over the years, and the earliest attempts approximated the BM by a damped mass-spring system and simplified the cochlear fluid dynamics significantly; for example, the steady potential flow model in [14]. More recent efforts have focused on incorporating more realistic fluid dynamics [2, 16, 20] as well as the complex interactions of the mechanical and cellular structures making up the cochlear partition [5, 17]. When the focus is on the cochlear fluid dynamics, one method that has proven particularly effective in capturing the effects of fluid-structure interaction is the immersed boundary method [5, 6, 12] – and this is the approach that we will employ in this paper. This study is motivated by three observations:

1. Direct experimental evidence that outer hair cells (OHC) embedded within the cochlear partition experience periodic contractions in response to BM oscillations [8, 9];
2. The suggestion by several authors that OHC contractions can modulate the BM stiffness [13, 15];

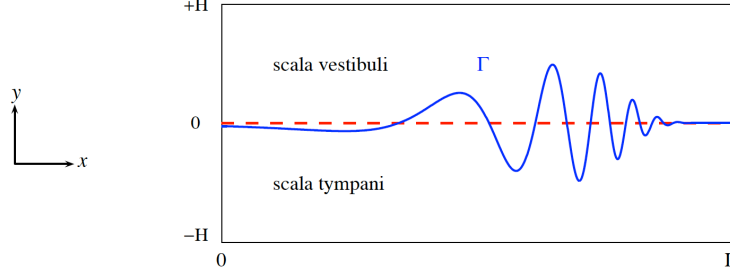


**FIGURE 1.** The cochlear duct is a rectangular fluid-filled domain of length  $L$  and height  $2H$  (the vertical scale is exaggerated since  $H \ll L$ ). The basilar membrane (denoted  $\Gamma$ ) has a flat equilibrium state  $y = 0$  shown as a dashed line.

3. A mathematical study of a fluid-structure interaction problem in which an internally-forced membrane (with a time-varying elastic stiffness) interacting with a viscous fluid gives rise to *parametric resonance* instabilities.

Our hypothesis is that the periodic internal forcing due to OHC oscillations in the basilar membrane can lead to parametric resonances that are mediated by cochlear hydrodynamics. We argue that the existence of such resonant instabilities constitutes a novel physical mechanism that has not yet been considered in connection with the cochlear active process. We develop a simple 2D immersed boundary model of a parametrically-excited BM and the surrounding cochlear fluid, perform a stability analysis that identifies parameter ranges over which resonances exist, and then provide numerical simulations that validate the results. More details of the model and the analytical and numerical results can be found in [10, 11].

## METHODS

### Immersed Boundary Model of the Basilar Membrane

Since our focus is on the fluid-structure interactions in the cochlea we will make use of the immersed boundary method, specifically the 2D model developed by LeVeque et al. [12]. They treated the fluid-filled cochlear duct as a rectangular domain of length  $L = 3.5$  cm, and the basilar membrane (BM, along with the cochlear partition in which it is embedded) as an elastic structure that divides the domain vertically into two fluid regions (the scala vestibuli and scala tympani). The fluid obeys the incompressible Navier-Stokes equations

$$\rho \frac{\partial \mathbf{u}}{\partial t} + \rho \mathbf{u} \cdot \nabla \mathbf{u} = -\nabla p + \mu \Delta \mathbf{u} + \mathbf{f}, \quad (1)$$

$$\nabla \cdot \mathbf{u} = 0, \quad (2)$$

where the fluid velocity is  $\mathbf{u}(\mathbf{x}, t)$   $\text{cm s}^{-1}$ , pressure is  $p(\mathbf{x}, t)$   $\text{g cm}^{-1} \text{s}^{-2}$ , density is  $\rho = 1.0 \text{ g cm}^{-3}$  and viscosity is  $\mu = 0.02 \text{ g cm}^{-1} \text{s}^{-1}$ . The rectangular cochlear duct is represented by points  $\mathbf{x} = (x, y) \in [0, L] \times [-H, H]$ , whereas the BM location is denoted  $\mathbf{X}(s, t)$  with  $s \in [0, L]$  a Lagrangian coordinate and  $\mathbf{X}_0(s) := (s, 0)$  representing the horizontal equilibrium state (refer to Fig. 1).

The fluid-structure interaction requires first that the membrane moves with the fluid in which it is immersed (the no-slip condition)

$$\frac{\partial \mathbf{X}}{\partial t}(s, t) = \mathbf{u}(\mathbf{X}(s, t), t) = \int_{-H}^H \int_0^L \mathbf{u}(\mathbf{x}, t) \delta(\mathbf{x} - \mathbf{X}(s, t)) dx dy, \quad (3)$$

where  $\delta(\mathbf{x})$  is the two-dimensional Dirac delta function. In turn, the BM exerts a singular elastic force

$$\mathbf{f}(\mathbf{x}, t) = \int_0^L K(s, t) (\mathbf{X}_0(s) - \mathbf{X}(s, t)) \delta(\mathbf{x} - \mathbf{X}(s, t)) ds, \quad (4)$$

on the surrounding fluid, which is simply a “spring-like” restoring force that drives points on the BM towards their equilibrium configuration  $\mathbf{X}_0$ . The function  $K(s, t)$  is the corresponding spring constant or stiffness, which we assume

to have the form

$$K(s, t) = \sigma e^{-\lambda s} (1 + 2\tau \sin(\omega t)), \quad (5)$$

where  $\sigma = 6 \times 10^5 \text{ g cm}^{-2} \text{ s}^{-2}$  is an elastic stiffness constant and  $\lambda = 1.4 \text{ cm}^{-1}$  captures the exponential rate of decrease in stiffness with length, taken in [12] based on von Békésy's experimental measurements of the human cochlea [21]. The time-dependent factor with dimensionless amplitude  $\tau \in [0, \frac{1}{2}]$  and frequency  $\omega \text{ (s}^{-1}\text{)}$  encapsulates the parametric forcing from OHC expansion/contraction that is a response to BM oscillations [8].

Numerical simulations are performed using a finite difference discretization of the above equations, where the fluid variables are approximated on an equally-spaced rectangular grid while the BM position is tracked on a set of moving points. Centered finite differences are used to approximate all derivatives, the delta functions are replaced with a smooth regularization, and the Navier-Stokes equations are solved using a split-step projection method that is described in detail in [10].

## Floquet Stability Analysis

The partial differential equations (PDEs) derived in the previous section are an example of a parametrically-forced system, in which the dynamics are driven by periodic variations in the parameter  $K(s, t)$ . This PDE system can be thought of as a generalization of the classical *damped Mathieu equation*, which is an ordinary differential equation model that arises from a variety of physical systems such as an inverted pendulum with a vibrating support, or a frequency-modulated audio signal carrier. Applying techniques from Floquet theory one can show that in contrast with externally-forced systems (where damping always stabilizes the dynamics), a small-amplitude internal or parametric forcing term can lead to unbounded oscillations in the solution, even in the presence of damping [3].

A similar Floquet analysis can be applied to our BM model equations, which we will only summarize briefly here and refer the interested reader to the paper [11] for complete details. First of all, because the amplitude of the BM oscillations is small in relation to  $L$ , we can linearize the equations of motion and take the BM displacement to be  $\mathbf{X} = (0, h(x, t))$ . The Floquet theory supposes a solution of the form

$$h(x, t) = e^{\gamma t} \sum_{n=-\infty}^{\infty} \sum_{k=-\infty}^{\infty} h_k^n e^{int} e^{ikx}, \quad (6)$$

where  $\gamma \in \mathbb{C}$  and  $\text{Re}(\gamma)$  determines the stability of the solution as  $t \rightarrow \infty$  (with similar expressions for the velocity and pressure). Substituting this series expansion into the governing equations yields an infinite linear system for  $h_k^n$

$$\left( \frac{2\pi^3 \mu^2}{\rho \sigma L^3 k} \right) \beta_k^n (\beta_k^n - k) (\beta_k^n + k)^2 h_k^n + \sum_{j=-\infty}^{\infty} c_{k-j} h_j^n = i\tau \sum_{j=-\infty}^{\infty} c_{k-j} (h_j^{n-1} - h_j^{n+1}) \quad (k, n \in \mathbb{Z}), \quad (7)$$

where  $\beta_k^n := \left( k^2 + \frac{\rho}{\mu} (\gamma + in) \right)^{1/2}$  and  $c_{k-j}$  are the Fourier coefficients of the factor  $e^{-\lambda|x|}$  in the BM stiffness (extended as an even periodic function of  $x$ ). This system can be written in the form of a generalized eigenvalue problem

$$\mathbf{A}\mathbf{h} = \tau\mathbf{B}\mathbf{h}, \quad (8)$$

where  $\tau$  is the eigenvalue,  $\mathbf{h} = (h_k^n)$  is the eigenvector of unknown coefficients, and  $\mathbf{A}, \mathbf{B}$  are (infinite) matrices with coefficients depending only on the physical parameters. By truncating the series expansions at a finite number of terms in  $j, k, n$ , the resulting finite system can be solved for the forcing amplitude  $\tau$  and the coefficients  $h_k^n$ .

Our main objective is to understand the underlying stability of solutions and to identify parameter values for which parametric resonance will occur. We therefore restrict our attention to marginally stable solutions satisfying  $\text{Re}(\gamma) = 0$ , and in the context of Floquet theory it is sufficient to consider only two values of  $\gamma$  corresponding to harmonic ( $\gamma = 0$ ) and subharmonic ( $\gamma = \frac{1}{2}i$ ) solutions.

## RESULTS

We now demonstrate the applicability of our model and the stability analysis by way of three examples: a parametrically-forced pure-tone response that exhibits travelling wave solutions consistent with other BM models; classical ‘‘Mathieu-type’’ instabilities that arise when the periodically-varying BM stiffness is uniform along its length ( $\lambda = 0$ ); and the analogous resonant instabilities that ensue when  $\lambda > 0$  causing the modes to be spatially-coupled.

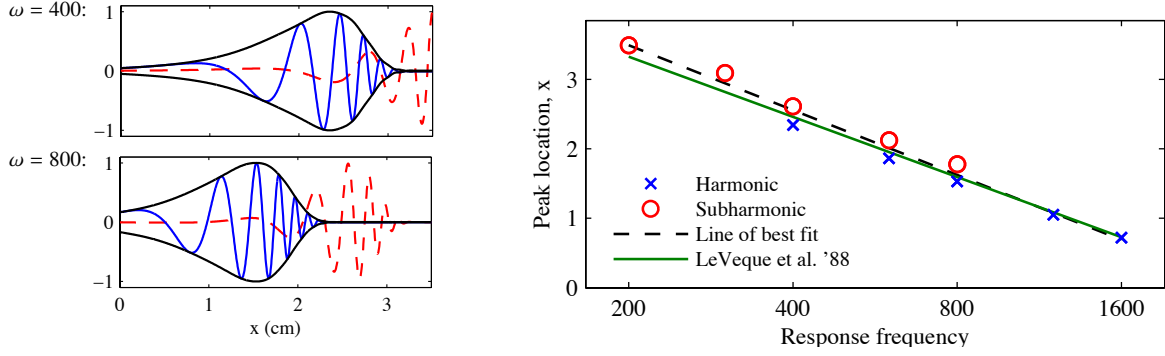


**FIGURE 2.** Left: Plots of pure-tone response for frequencies  $\omega = 400$  (top) and  $800 \text{ s}^{-1}$  (bottom), showing the harmonic (solid line) and subharmonic (dashed line) solutions. Right: Analytical BM peak locations compared with results from LeVeque et al. [12].

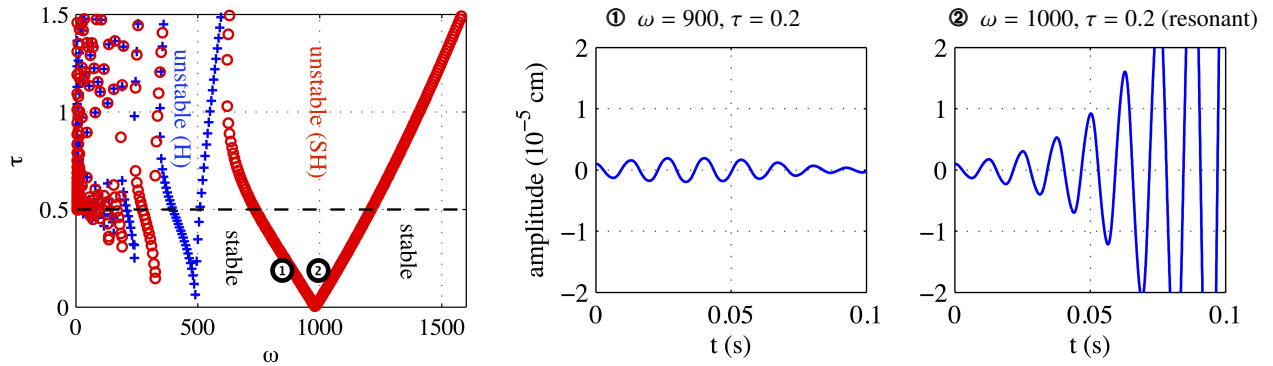


**FIGURE 3.** BM parametric resonance instability for the  $k = 1$  mode with constant stiffness ( $\lambda = 0$ ). Left: Stability plot showing unstable tongues and highlighting two sets of parameters: one stable ① and one unstable ②. Middle, right: Numerical solutions of peak BM amplitude for the same stable and unstable modes.

### Parametrically-Forced Pure Tone Response

Here we solve the eigenvalue problem (7) numerically and select the resonant solution mode corresponding to the smallest value of  $\tau$ , which is incidentally also the dominant  $k = 1$  mode. The BM profile is then constructed using (6) and compared to the travelling wave solutions obtained by LeVeque et al. [12] in response to a pure-tone external forcing. The results for two forcing frequencies  $\omega = 400, 800 \text{ s}^{-1}$  are presented in Fig. 2(left), and the envelope of the harmonic model has the typical asymmetric wave shape observed in experiments and other models [5, 17, 18]. The subharmonic mode has a similar shape, except that the response occurs at a frequency equal to one-half that of the internal forcing so that the wave profiles appear shifted relative to the harmonic solution (therefore, the location of the BM peak depends on the response frequency and not the forcing frequency). Figure 2(right) shows that the peak locations match closely with the analytical results in [12] as well as capturing the well-known logarithmic dependence on frequency that was first observed by von Békésy [21].

### Constant BM Stiffness ( $\lambda = 0$ )

The primary difference between the Floquet solution (7) and that for the classical Mathieu equation is that the spatial dependence in the BM elastic stiffness (5) couples together all spatial modes  $k$ , which complicates the analytical solution significantly. We therefore start by considering the trivial case of a BM with homogeneous stiffness ( $\lambda = 0$ ), where the eigenvalue problems decouple and yield a discrete sequence of real eigenvalues for each wavenumber  $k$ . These modes are easily visualized by means of a plot of the forcing amplitude  $\tau$ , which trace out curves in parameter space that separate stable from unstable solutions. A plot of  $\tau$  versus forcing frequency is shown in Fig. 3 for the dominant  $k = 1$  mode, which exhibits stability boundaries having the characteristic shape of “unstable tongues”

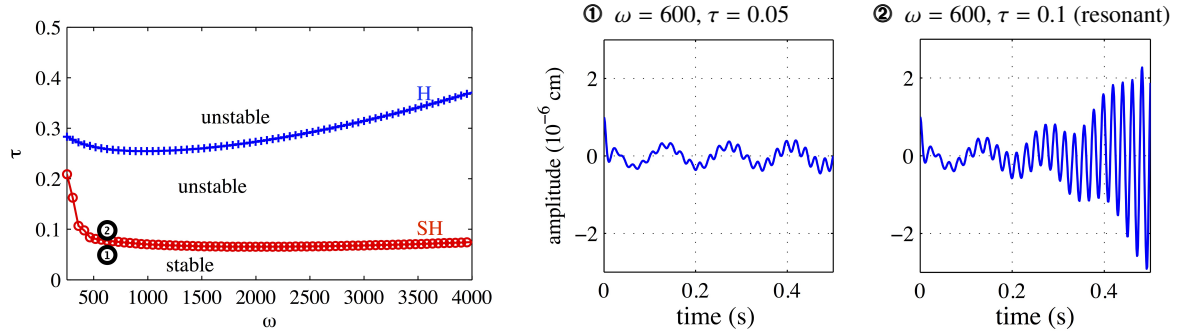


**FIGURE 4.** BM instability for spatially-varying stiffness with  $\lambda = 1.4$ . Left: Stability diagram showing that over most of the audible hearing range. Middle, right: Comparison of BM amplitude for the  $k = 1$  mode at frequency  $\omega = 600 \text{ s}^{-1}$ , corresponding to ① a stable solution with  $\tau = 0.05$  and ② a resonant solution with  $\tau = 0.1$ .

extending downward to the  $\tau = 0$  axis and alternating between harmonic and subharmonic solutions. Plots of the maximum BM amplitude are provided in Fig. 3(middle, right) for two sets of parameters corresponding to stable and resonant solutions, which demonstrate that the predicted stability boundaries are indeed relatively sharp.

### Exponentially-Varying BM Stiffness

When we let the BM stiffness vary exponentially with length, taking  $\lambda = 1.4$ , a “mode-mixing” effect occurs and the stability plot is a simultaneous overlap of the unstable “tongues” for all wavenumbers. Therefore, for each any given set of parameter values, we select the smallest eigenvalue  $\tau$  for all  $k$  and use that as a measure of the dominant unstable mode. The resulting stability region is plotted against a wide range of audible frequencies in Fig. 4(left), which shows that the marginal stability curve can be described by a function of the form  $\tau = g(\omega)$ ; in particular, we note that an unstable subharmonic mode exists whenever the parametric forcing satisfies  $\tau \gtrsim 0.08$  (except for sound frequencies at the lower end of the audible range). Again, we present two numerical simulations of the PDE model in Fig. 4(right) for parameters on either side of the stability boundary, in order to demonstrate that the analysis provides a sharp estimate of the onset of resonant instabilities.

Experimentally measured values of stiffness  $\sigma$  that are reported in the literature for human cochleas exhibit a large variation, ranging from the value  $6 \times 10^5$  (which we used above to allow a direct comparison with results in [12]) to as high as  $2 \times 10^9$  (from [14] and other sources). Our model yields similar stability results over this entire range of stiffness as well as for parameters  $(L, \lambda, \sigma)$  corresponding to other mammalian cochleas such as the gerbil [11] where we obtain qualitatively similar results. The contour plot in Fig. 5 displays the minimum value of the forcing amplitude  $\tau$  that yields resonant solutions over a fairly wide range of stiffness and frequency relevant to the human cochlea. Except for a small parameter region (in the lower right) corresponding to low stiffness and high frequency, parametric resonances appear to persist over most of the physiological range. Clearly though, the forcing amplitude actually generated by OHCs may not be sufficient to generate a particular unstable mode, and so this is something that would require further study involving actual BM stiffness modulations measured in experiments.

## DISCUSSION

In contrast with most other mathematical models of the cochlear active process that incorporate the effect of OHC oscillations using an *external forcing* term, we consider the subsequent generation of periodic modulations in the BM stiffness which takes the form of an *internal force*. This model not only reproduces the typical travelling-wave solutions for a passive BM, but also indicates the existence of instabilities arising from the fluid-structure interaction – this is a new physical mechanism that has until now not been considered in the hearing literature. These instabilities can develop even under the influence of fluid viscosity, provided that the amplitude of the BM stiffness oscillations is large enough, specifically  $\tau \gtrsim 0.08$  for parameters corresponding to the human cochlea. This type of instability is generic and persists over a wide range of frequencies and stiffness parameters relevant to mammalian hearing systems (including humans and guinea pigs).

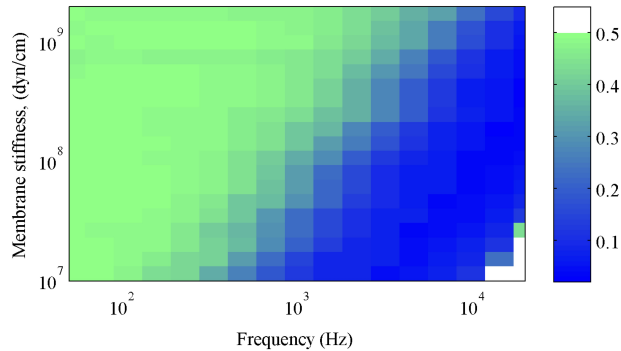


**FIGURE 5.** Minimum forcing amplitude  $\tau$  required for there to exist at least one resonant mode with a range of BM stiffness and sound frequency parameters that are relevant to the human cochlea.

This leads us to hypothesize that hydrodynamically-driven parametric resonance instabilities could have a significant impact on cochlear amplification, and so are worthy of further study. Because of the mode-mixing effect arising from the spatially-dependent nature of the BM stiffness, there is no obvious “signature” that can be used to identify the existence of this instability in experiments (as there is for the simpler Mathieu equation). Instead, we are currently extending our model to couple these fluid-structure interactions along with another more well-accepted model for the cochlear active process (for example, those in [13, 17]) in order to evaluate the relative importance of hydrodynamically-mediated resonant interactions with other physical mechanisms. Our hope is that this study will identify a signature of parametric resonance that can then be investigated experimentally. Another more easily testable hypothesis is whether the variations in BM stiffness that are induced by OHC oscillations (according to [13, 15]) have an amplitude that satisfy the requirement  $\tau \gtrsim 0.08$ , which our analysis indicates is needed to observe parametric resonances. Finally, the mathematical framework we have developed here is well-suited for studying the fluid mechanics of other aspects of cochlear mechanics such as oscillatory fluid flows in the tunnel of Corti [9], or the flow-induced coupling to oscillations of the Reissner’s membrane [19].

## ACKNOWLEDGMENTS

This work was supported by a Discovery Grant from the Natural Sciences and Engineering Research Council of Canada.

## REFERENCES

- [1] Allen JB, Nakajima HH, Ó Maoiléidigh D (2015) Middle ear mechanics and progress in cochlear modeling: A moderated discussion. In: Karavitaki KD, Corey DP (eds) *Mechanics of Hearing: Protein to Perception*, AIP Conference Proceedings 1703:060007
- [2] Ashmore J et al. (2010) Editorial: The remarkable cochlear amplifier. *Hearing Res* 266(1-2):1–17
- [3] Champneys AR (2009) The dynamics of parametric excitation. In: Meyers RA (ed) *Encyclopedia of Complexity and Systems Science*, New York: Springer, pp. 2323–2344
- [4] Dallos P (1992) The active cochlea. *J Neurosci* 12(12):4575–4585
- [5] Edom E, Obrist D, Henniger R, Kleiser L, Sim, JH, Huber AM (2013) The effect of rocking stapes motions on the cochlear fluid flow and on the basilar membrane motion. *J Acoust Soc Am* 134(5):3749–3758
- [6] Givelberg E, Bunn J (2003) A comprehensive three-dimensional model of the cochlea. *J Comput Phys* 191(2):377–391
- [7] Hudspeth AJ (1997) Mechanical amplification of stimuli by hair cells. *Curr Opin Neurobiol* 7:480–486
- [8] Hudspeth AJ (2008) Making an effort to listen: Mechanical amplification in the ear. *Neuron* 59(4):530–545
- [9] Karavitaki KD, Mountain DC (2007) Evidence for outer hair cell driven oscillatory fluid flow in the tunnel of Corti. *Biophys J* 92(9):3284–3293

- [10] Ko W (2015) Parametric resonance in immersed elastic structures, with application to the cochlea. PhD thesis, Department of Mathematics, Simon Fraser University, Burnaby, Canada.
- [11] Ko W, Stockie JM (2015) An immersed boundary model of the cochlea with parametric forcing. *SIAM J Appl Math* 75(3):1065–1089
- [12] LeVeque RJ, Peskin CS, Lax PD (1988) Solution of a two-dimensional cochlea model with fluid viscosity. *SIAM J Appl Math* 48(1):191–213
- [13] Markin VS, Hudspeth AJ (1995) Modeling the active process of the cochlea: Phase relations, amplification, and spontaneous oscillation. *Biophys J* 69(1):138–147
- [14] Neely ST (1981) Finite difference solution of a two-dimensional mathematical model of the cochlea. *J Acoust Soc Am* 69(5):1386–1393
- [15] Nilsen KE, Russell IJ (1999) Timing of cochlear feedback: spatial and temporal representation of a tone across the basilar membrane. *Nature Neurosci* 2(7):642–648
- [16] Ramamoorthy S, Deo NV, Grosh K (2007) A mechano-electro-acoustical model for the cochlea: Response to acoustic stimuli. *J Acoust Soc Am* 121(5):2758–2773
- [17] Reichenbach T, Hudspeth AJ (2010) A ratchet mechanism for amplification in low-frequency mammalian hearing. *Proc Nat Acad Sci USA* 107(11):4973–4978
- [18] Reichenbach T, Hudspeth AJ (2014) The physics of hearing: Fluid mechanics and the active process of the inner ear. *Rep Prog Phys* 77:076601
- [19] Reichenbach T, Stefanovic A, Nin F, Hudspeth AJ (2012) Waves on Reissner’s membrane: A mechanism for the propagation of otoacoustic emissions from the cochlea. *Cell Rep* 1(4):374–384
- [20] Shera CA, Tubis A, Talmadge CL (2005) Coherent reflection in a two-dimensional cochlea: Short-wave versus long-wave scattering in the generation of reflection-source otoacoustic emissions. *J Acoust Soc Am* 118(1):287–313
- [21] von Békésy G (1960) *Experiments in Hearing*. New York: McGraw Hill